MRS Communications (2016), 6, 9–15
© Materials Research Society, 2015
doi:10.1557/mrc.2015.84

MRS Communications

Plasmonics, Photonics, and Metamaterials Research Letter

Low-loss silicon wire waveguides for optical integrated circuits

Tsuyoshi Horikawa*, Photonics Electronics Technology Research Association (PETRA), 16-1 Onogawa, Tsukuba 305-8569, Japan; National Institute of Advanced Industrial Science and Technology (AIST), 16-1 Onogawa, Tsukuba 305-8569, Japan
Daisuke Shimura, and **Tohru Mogami,** Photonics Electronics Technology Research Association (PETRA), 16-1 Onogawa, Tsukuba 305-8569, Japan
*Address all correspondence to Tsuyoshi Horikawa at **tsuyoshi.horikawa@aist.go.jp**

(Received 14 October 2015; accepted 14 December 2015)

Abstract

Low-propagation-loss silicon wire waveguides are key components of optical integrated circuits. In this paper, we clarified, through assessment of the relationship between waveguide loss and fabrication technology that high-resolution lithography and an adjusted lithography process window are important for low-loss waveguides. The silicon wire waveguides fabricated by high-resolution lithography technology using ArF immersion lithography process showed world-record low propagation losses of 0.40 dB/cm for the C-band and 1.28 dB/cm for the O-band. Analysis with Barwicz and Haus's theory indicated that sidewall scattering is the main cause of propagation loss even in such low-loss waveguides.

Introduction

Optical integrated circuits using silicon photonics technology have been expected to be a solution to the bandwidth bottleneck problem both in data transmission among large scale integration (LSI) circuits and in long-haul communication.[1–3] A silicon photonics transceiver for the above communication consists of a continuous-wave light source array and optical modulator array in the transmitter circuit and a photodetector array in the receiver circuit.[4,5] Silicon waveguides of rib type[4] or wire type[5] structure are used to optically connect these devices. The wire waveguide has the advantage of lower emission loss at a corner with a short bending radius because the propagating light in wire waveguides is more strongly confined in the waveguide core. Using the wire waveguides has made it possible to make optical transceivers with a footprint of only several tens of square millimeters.[5] The problem with the wire waveguides is their relatively higher propagation loss. The propagation loss of wire waveguides has been reported to be a few decibels per centimeter,[6–20] whereas that of rib waveguides has been reported to be <0.5 dB/cm.[21] The higher power consumption due to this larger propagation loss makes it difficult to design large-scale circuits using the wire waveguides. Many intensive studies have been devoted to reducing the propagation loss of wire waveguides, and recently research groups at IMEC[15,19] and PETRA[20] have independently reported wire waveguides with propagation losses <1.0 dB/cm. In the "Recent development of low-loss silicon wire waveguides" section, we will briefly review the previous studies and describe the key issues in lowering the propagation loss of a wire waveguide.

As for the loss mechanism in wire waveguides, in 1994 Payne and Lacey derived an analytical equation, on the basis of two-dimensional (2D) analysis, that exhibits strong dependence on line edge roughness (LER)[22]; and in 2005, Barwicz and Haus reported the results of a more accurate three-dimensional (3D) simulation.[23] It will be interesting to see whether the propagation loss in recently developed low-loss waveguides can be explained by these theories, the examination of which will help us better understand the propagation loss mechanism.

One purpose of this paper is to show a solution to the problem of lowering propagation loss through assessment of the relationship between waveguide loss and fabrication technology in the previous studies. A second purpose is to describe the propagation characteristics of the low-loss waveguides and compare them with the results of simulations based on different scattering loss theories.

Recent development of low-loss silicon wire waveguides

The typical cross-sectional structure of a wire waveguide and a bird's-eye view of the waveguide core pattern are shown in Fig. 1. Silicon core patterns for wire waveguides with submicrometer width are fabricated by resist pattern formation by lithography on a silicon layer on a thick buried oxide (BOX) and the following anisotropic dry etching of the silicon layer. This fabrication flow for silicon photonics waveguides using silicon on insulator (SOI) wafers with thick BOX was established in the early stage, up to the year 2005.[6–10] In this period, several papers confirmed experimentally that the scattering of propagating light by LER is the main cause of the propagation loss,[6,8] and the sidewall striation like that seen in Fig. 1(b) was been found to be the main origin of LER. Table I shows the main results of propagation loss

https://doi.org/10.1557/mrc.2015.84 Published online by Cambridge University Press

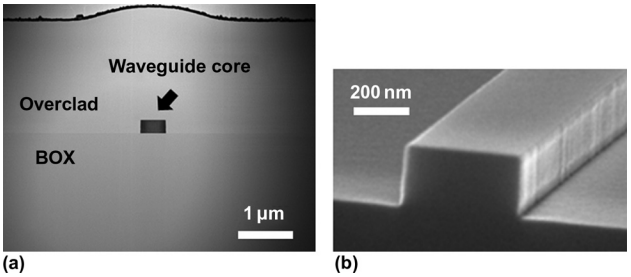


Figure 1. (a) Cross-sectional structure of a wire waveguide and (b) bird's-eye view of the waveguide before formation of the overclad layer.

reported from 2004 to the present. The waveguide loss <2 dB/cm for the propagation in the lowest-order transverse electric (TE) mode was first reported in 2006 by the IBM group, which used thermal oxidation for sidewall smoothing after waveguide pattern formation.[11] The first loss <1 dB/cm was reported in 2008 by the University Glasgow group, which used hydrogen silsesquioxane as a negative-tone electron-beam (EB) resist.[12] The impact of resist chemistry on the propagation loss has been also reported in a negative-tone chemically amplified EB resist, OEBR-CAN034.[16] In 2012, an IMEC group reported a loss <1 dB/cm obtained using ArF immersion lithography.[15] It is noteworthy that in the research works by the IMEC group,[9,14,15,19] the propagation loss was reduced using higher-resolution lithography. Nowadays a propagation loss <2 dB/cm is commonly obtained in major silicon photonics platforms including foundries.[24] Loss values <1 dB/cm, however, have been reported only by the above three groups. The results listed in Table I make it clear that the lithographic process greatly impacts the propagation loss.

Table II shows the comparison of the photolithography tools in the resolution of photolithography for silicon photonics as

Table I. Comparison of propagation losses for the lowest-order TE mode reported for silicon wire waveguides.

Ref.	Year	Lithography	Width	Height	λ (nm)	α (dB/cm)
[6]	2004	EB	445	220	1500	3.6
[7]	2005	KrF	500	200	1425–1575	~5
[8]	2005	KrF	630	220	1550	1.9
[9]	2005	KrF	400	220	1550	34
			450	220	1550	7.4
			500	220	1550	2.4
[10]	2005	EB	480	200	1550	1.18
[11]	2007	EB	510	226	1550	1.7
[12]	2008	EB	500	260	1520–1525	0.92
[13]	2008	EB	480	200	1550	1.18
[14]	2010	ArF	460	220	1550	2.7
[15]	2012	ArF-I	457	220	1550	0.71
[16,17]	2012	EB	440	220	1550	1.2–1.8
[17,18]	2012	ArF-I	440	220	1550	1.2–1.8
[19]	2014	ArF-I	400	220	1550	0.8
			450	220	1550	0.74
			500	220	1550	0.5
[20]	2014	ArF-I	440	220	1550	<0.5
[5]	*2015*	EB	*348*	*200*	*1310*	*~3*
This work		ArF-I	440	220	1550	0.40
		ArF-I	*320*	*220*	*1310*	*1.28*

EB, electron beam lithography; KrF, KrF excimer lithography (λ = 248 nm); ArF, ArF excimer lithography (λ = 193 nm); ArF-I, ArF immersion lithography (λ = 193 nm). The propagation loss data for the O-band is indicated by an italic font.

https://doi.org/10.1557/mrc.2015.84 Published online by Cambridge University Press

well as the resolution for CMOS devices.[25] In the estimation of the resolution for silicon photonics, we supposed the annular condition as the off-axis illumination condition because higher-resolution conditions such as dipole and quadrupole illumination are not suitable for irregular waveguide patterns. In this illumination condition, the lithographic resolutions for KrF, ArF, and ArF immersion lithography were estimated to be 150, 110, and 70 nm, respectively. It was confirmed that the difference in resolution by lithography tools due to the wavelength of exposure light and numerical aperture (*NA*) also causes differences in LER. Smoothing techniques such as oxide formation on waveguides surface after pattern formation are also effective to a certain extent, although these techniques cause a little change of waveguide size.

Propagation loss in wire waveguides fabricated using ArF immersion lithography

Two types of wire waveguides (waveguides ***A*** and ***B***) with different widths and heights were fabricated using 300-mm-diameter SOI wafers having a 2-μm-thick BOX layer. The SOI thickness uniformity within a single wafer and the surface roughness determined by atomic force microscope measurement for 2 μm × 2 μm area were 0.27 nm (1σ) and 0.16 nm (1σ), respectively. The width and height of waveguide ***A*** were 440 and 220 nm, respectively, and the properties for the lowest-order TE mode propagation for the C-band (1.53–1.565 μm) were evaluated using the waveguide ***A***. The width and height of waveguide ***B***, on the other hand, were respectively 320 and 220 nm, and the waveguide ***B*** was tested for the lowest-order TE mode propagation for the O-band (1.26–1.36 μm). ArF immersion lithography was used as the lithography tool. We also used a half-tone mask with semi-transparent MoSi as the lithography mask because a half-tone mask gives a 0.3 nm smaller standard deviation of LER, σ_{LER}, than a binary mask does, due to the resolution improvement by optical interference with phase-shifted light.[26] From the standpoint of low LER pattern formation, we selected a high-resolution positive-tone chemically amplified photoresist. For an etching mask we used, a multi-layered mask structure including a photoresist layer and hard mask layers. The lithography process for waveguide pattern formation was optimized for minimizing LER and the shift of waveguide width. After resist pattern formation by photolithography process, the waveguide core pattern was formed by anisotropic dry etching, and then a 2-μm-thick SiO_2 film was deposited as a cladding layer.

Vertical sidewall of the waveguide core and quite small deviation from design in waveguide width and height were confirmed in the cross-section image for the fabricated waveguide by transmission electron microscopy (TEM) [Fig. 2(a)]. In our previous paper, regarding the fabrication errors in 440-nm-wide/220-nm-thick waveguides, it has been estimated that standard deviations in waveguide cross-sectional size for a single 300-mm wafer were confirmed to be 0.83 nm in width and 0.24 nm in height.[27] By the edge pattern analysis of a plan-view image for the waveguide core by scanning electron microscopy (SEM) [Fig. 2(b)], the value of σ_{LER} was evaluated to be 1.0 nm (1σ). Figure 3 shows the autocorrelation function analysis calculated using the waveguide edge pattern. The simulation curves with exponential autocorrelation functions [$R(u) = \sigma_{LER}^2$ EXP($-|u|/L_C$)] and Gaussian autocorrelation functions [$R(u) = \sigma_{LER}^2$ EXP($-|u|^2/L_C^2$)] are also plotted in Fig. 3, where L_C is a correlation length for LER. In the distance range <100 nm, the observed autocorrelation function almost agrees with the exponential autocorrelation function with L_C of 20 nm. We note that, in the comparison with the previous reports,[8,28] the estimated values of σ_{LER} of 1.0 nm and L_C of 20 nm are relatively low.

Typical test elements and measurement setup for propagation loss measurement are shown in Fig. 4. The amplified spontaneous emission light propagating through a single-mode fiber was optically coupled to waveguides by butt–joint coupling to a simple spot-size converter with a tapering-shaped waveguide. The coupling loss between the fiber and the spot-size converter is about 5 dB for the C-band and 4 dB for the O-band. To evaluate the transmittance for the waveguide with a given length, three devices with the same waveguide length in the same die on a single wafer were measured, and then we use the average value of them. The propagation loss per unit length was evaluated from slope in the dependence of transmission intensity on waveguide lengths. The evaluation of propagation loss was done for a several chips on two wafers fabricated by the

Table II. Performance comparison for photolithography tools of KrF excimer lithography (KrF), ArF excimer lithography (ArF), and ArF immersion lithography (ArF-I) in CMOS and silicon photonics fabrication.

Lithography	λ (nm)	*NA*	For CMOS		For silicon photonics	
			Illumination condition	Resolution (nm)	Illumination condition	Resolution (nm)
KrF	248	0.8	Dipole (line) CQuad (hole)	120	Annular	150
ArF	193	0.9	Dipole (line) CQuad (hole)	65	Annular	110
ArF-I	193	1.35	Dipole (line) CQuad (hole)	40	Annular	70

https://doi.org/10.1557/mrc.2015.84 Published online by Cambridge University Press

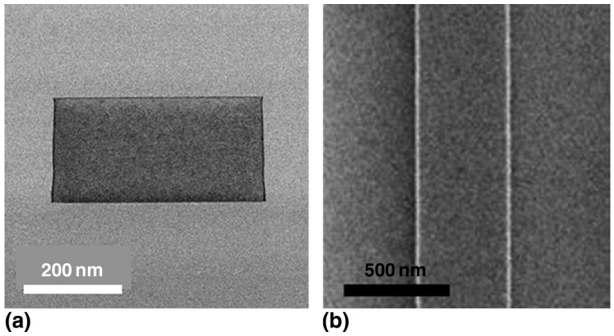


Figure 2. (a) TEM cross-section of the waveguide, and (b) SEM plain view of the waveguide core.

same fabrication flow. Because the values of the propagation loss for these chips agreed with each other within the experimental error, we used the results for the center chip on one wafer in the following description.

Figure 5(a) shows the dependence of transmission intensity on the length of the waveguide ***A*** (with a width of 440 nm and a height of 220 nm) for a wavelength of 1.55 μm. The propagation loss was evaluated to be 0.40 ± 0.06 dB/cm from the slope in linear fitting. The propagation loss spectra in the C-band for the waveguide are shown in Fig. 5(b). It was confirmed that the propagation loss was <0.5 dB/cm in the entire C-band (1.53–1.565 μm), although the loss gradually increases with the decrease of the wavelength in the range <1.52 μm.

Figure 6(a) shows the dependence of transmission intensity on the length of the waveguide ***B*** (with a width of 320 nm and a height of 220 nm) for a wavelength of 1.31 μm. The propagation loss was evaluated to be 1.28 ± 0.10 dB/cm. In the propagation loss spectra for the waveguide ***B*** [Fig. 6(b)], the propagation loss showed the minimum about 1.28 μm and was <1.8 dB/cm throughout the entire O-band (1.26–1.36 μm).

To the best of our knowledge, these obtained losses of 0.40 dB/cm for 1.55 μm and 1.28 dB/cm for 1.31 μm are the lowest

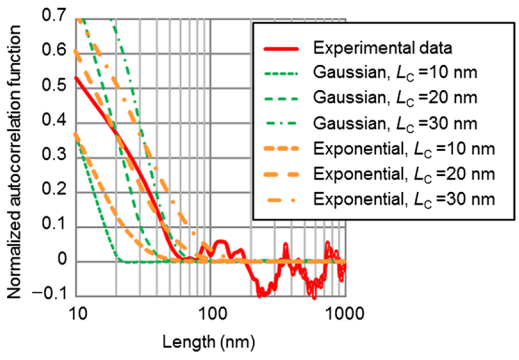


Figure 3. Autocorrelation function calculated using the waveguide edge pattern in Figure 2(b). Exponential-type and Gaussian-type theoretical curves are plotted in the graph.

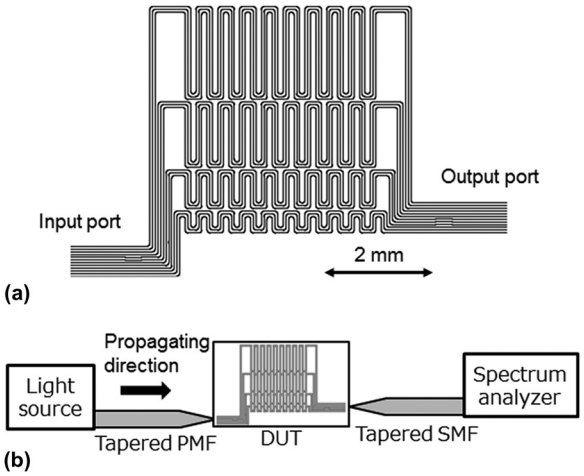


Figure 4. Typical test elements and measurement setup for propagation loss measurement.

propagation loss values for the lowest-order TE mode propagation in wire waveguides.

Propagation loss mechanism

The physical origin for the propagation loss of the wire waveguides can be classified into the following four categories: (1) absorption in the silicon core such as bulk absorption, (2) scattering at the interface between the silicon core and the clad, (3) absorption by impurities in the interface and the clad, and (4) optical leakage to the silicon substrate through BOX. The bulk absorption of non-doped silicon for 1.55 nm infrared light is quite small. Although it was reported that impurity absorption due to metal residue at the interface[29] and H_2O in clad[30] degrade the propagation properties, these factors can be eliminated by the careful cleaning of the waveguide surface and appropriate post-process design. Regarding optical leakage, the leakage of propagating light for the lowest-order TE mode propagation to the substrate was estimated to be a negligible value $<1 \times 10^{-4}$ dB/cm for a BOX thickness more than 1.5 μm.[31] Thus, it is considered that scattering at the interface between the silicon core and clad is the main cause of the propagation loss.

The analytical relationship between scattering loss $\alpha_{\mathrm{Scatter}}$ and σ_{LER} was derived by Payne and Lacey in the following forms using a 2D volume current method as a perturbation technique[22]:

$$\alpha_{\mathrm{Scatter}} = \frac{{\sigma_{\mathrm{LER}}}^2}{\sqrt{2}\, k_0\, n_{\mathrm{Si}} (w/2)^4} g(n_{\mathrm{eff}}, n_{\mathrm{Si}}, n_{\mathrm{clad}}, w) f(L_c), \qquad (1)$$

here k_0, n_{Si}, and w are a free-space wave number, the refractive index of silicon, and the waveguide width, respectively. Regarding the function g, although many normalized parameters were used in deviation in ref. 22, we here express the

https://doi.org/10.1557/mrc.2015.84 Published online by Cambridge University Press

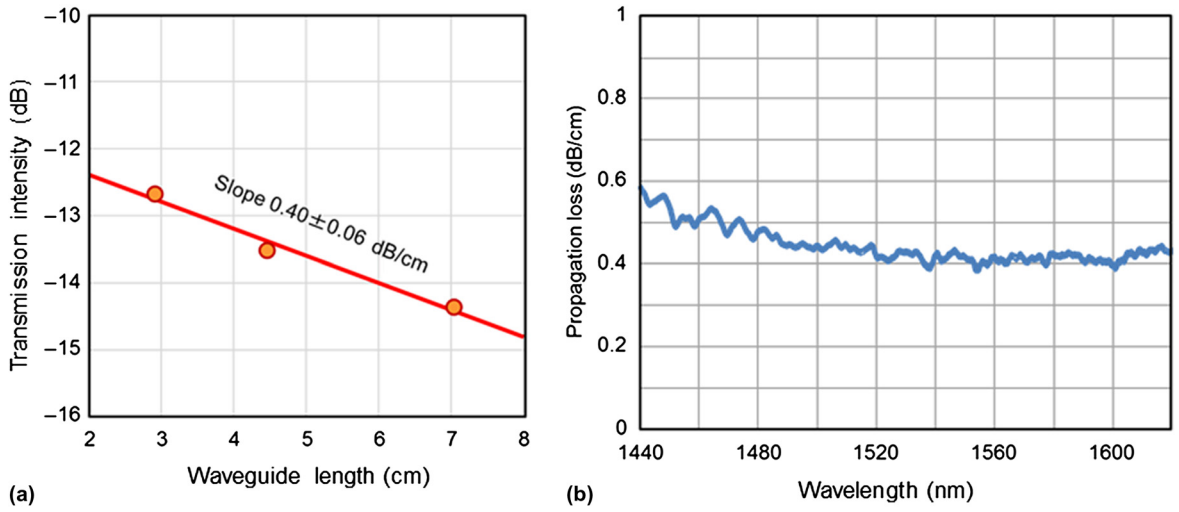


Figure 5. (a) The dependence of transmission intensity on the length of the waveguide ***A*** (440 nm wide and 220 nm high) for a wavelength of 1.55 μm, and (b) propagation loss spectra in the C-band for the waveguide ***A***.

function only using basic waveguide parameters in the following form:

$$g(n_{\mathrm{eff}}, n_{\mathrm{Si}}, n_{\mathrm{clad}}, w) \sim \frac{(w/2)^4 k_0^4 (n_{\mathrm{Si}}^2 - n_{\mathrm{eff}}^2)(n_{\mathrm{Si}}^2 - n_{\mathrm{clad}}^2)}{1 + (w/2)k_0\sqrt{n_{\mathrm{eff}}^2 - n_{\mathrm{clad}}^2}}, \quad (2)$$

here n_{eff} and n_{clad} are the effective refractive index of the waveguide and the refractive index of the clad, respectively. The value of g slowly varies with the parameters of the waveguides. Although $f(L_C)$ in Eq. (1) has a complicated form, and, for strong guiding waveguides, such as silicon wire waveguides, it can be approximated in the following form[22]:

$$f(L_c) \sim \frac{L_C k_0 \sqrt{2(n_{\mathrm{eff}}^2 - n_{\mathrm{clad}}^2)}}{1 + L_C^2 k_0^2 (n_{\mathrm{eff}}^2 - n_{\mathrm{clad}}^2)}, \quad (3)$$

here we expressed the function using only basic parameters and L_C. The $f(L_C)$ gradually increases with the increase of L_C for small L_C and has a maximum value at around $L_C \sim 120$ nm, for the waveguides with a width of 440 nm and height of 220 nm that were tested for the lowest-order TE mode propagation in the C-band.

The above analytical formula by Payne and Lacey was originally developed for silica-based waveguides in planar

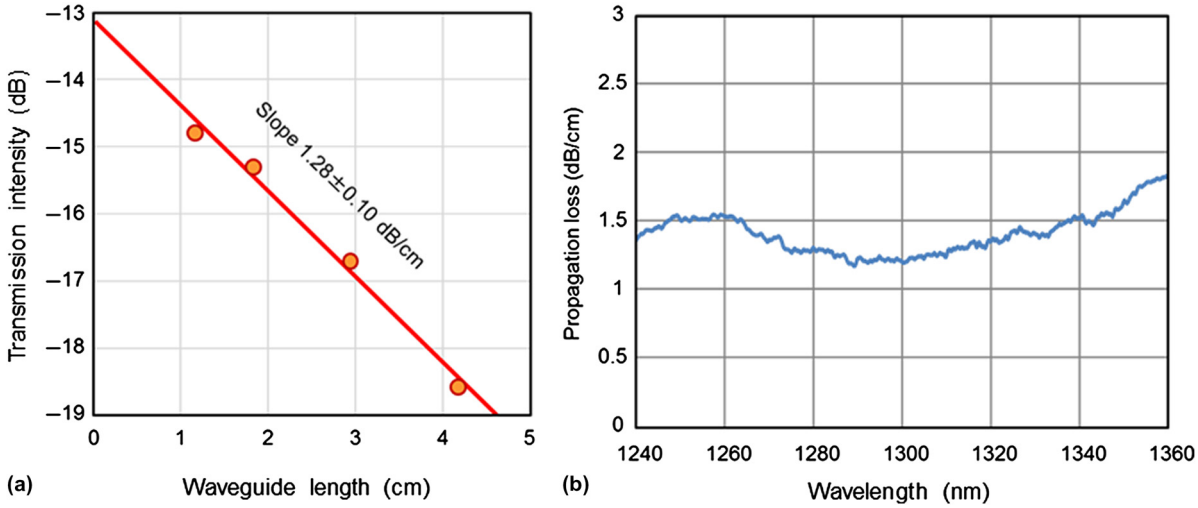


Figure 6. (a) The dependence of transmission intensity on the length of the waveguide ***B*** (320 nm wide and 220 nm high) for a wavelength of 1.31 μm, and (b) propagation loss spectra in the O-band for the waveguide ***B***.

https://doi.org/10.1557/mrc.2015.84 Published online by Cambridge University Press

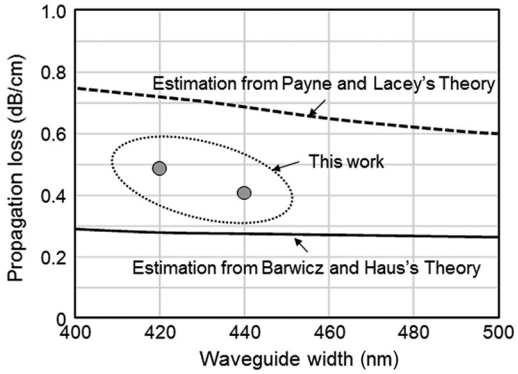


Figure 7. The dependence of the propagation loss in C-band for the waveguide ***A*** on the waveguide width. The simulation results by Payne and Lacy theory and Barwick's theory were also plotted.

lightwave circuits (PLCs). In the quantitative comparison with experimental data for high-index-contrast silicon waveguides, it has been reported that their theory tends to overestimate the scattering loss.[30] Barwicz and Haus recently developed a 3D simulation technique for rectangular-shape waveguides using a 3D volume current method.[23] Although no simple analytical formulation exists in their simulation, they presented useful graphs showing the relationship between LER and scattering loss for three core materials: SiON, SiN, and Si.

In this paper, we compare our experimental results with the corresponding values estimated using the above two theories. Figure 7 shows the dependence of the propagation loss for the C-band in sample **A** and also shows the simulation results obtained with Payne and Lacey's theory and Barwicz and Haus's theory. In the simulation, the roughness parameters evaluated in this study, σ_{LER} of 0.97 nm and L_C of 20 nm, were used. It is confirmed that Payne and Lacey's theory also overestimates loss in our case, whereas Barwicz and Haus's theory exhibits loss values lower by 0.1–0.2 dB/cm than the experimental loss for our waveguides. This implies that scattering loss which obeys Barwicz and Haus's scattering theory is the main cause even for quite low loss waveguides, and some of the measured loss may have another physical origin. Further experiments and analysis should be done in order to clarify the propagation loss mechanism in low-loss wire waveguides.

Conclusions

Low-propagation-loss silicon wire waveguides are key components for making large-scale optical integrated circuits with a small footprint. This paper has discussed fabrication requirements for low-loss waveguides through the assessment of the relationship between waveguide loss and fabrication technology in previous studies. The importance of high-resolution lithography and an adjusted lithography process window was pointed out. The propagation characteristics of the low-loss waveguides fabricated using ArF immersion lithography were described. As for the propagation performance of the waveguides, rectangular silicon waveguides 440 nm wide and 220 nm high showed a low propagation loss of 0.40 dB/cm in the lowest-order TE mode propagation for a wavelength of 1.55 μm. A low propagation loss of 1.28 dB/cm was also confirmed for 320-nm-wide, 220-nm-height waveguides for a wavelength 1.31 μm. The analysis with Barwicz and Haus's theory indicated that sidewall scattering is the main cause of propagation loss even in such low-loss waveguides. These high-performance wire waveguides contribute to realizing the low-operation-power optical circuits using silicon photonics technology for data communication.

Acknowledgments

This research was partly supported by the New Energy and Industrial Technology Development Organization (NEDO). The authors thank Mr. M. Seki, National Institute of Advanced Industrial Science and Technology (AIST), for his valuable information and discussion about ArF immersion lithography technology.

References

1. Y.A. Vlasov: Silicon CMOS-integrated nano-photonics for computer and data communications beyond 100G. *IEEE Commun. Mag.* **50**, s67 (2012).
2. M. Zuffada: The industrialization of the Silicon Photonics: Technology roadmap and application (Proc. European Solid-State Device Res. Conf., Milan, Italy, 2012) p. 7.
3. Y. Arakawa, T. Nakamura, Y. Urino, and T. Fujita: Silicon photonics for next generation system integration platform. *IEEE Commun. Mag.* **51**, 72 (2013).
4. F. Boeuf, S. Cremer, N. Vulliet, T. Pinguet, A. Mekis, G. Masini, L. Verslegers, P. Sun, A. Ayazi, N.-K. Hon, S. Sahni, Y. Chi, B. Orlando, D. Ristoiu, A. Farcy, F. Leverd, L. Broussous, D. Pelissier-Tanon, C. Richard, L. Pinzelli, R. Beneyton, O. Gourhant, E. Gourvest, Y. Le-Friec, D. Monnier, P. Brun, M. Guillermet, D. Benoit, K. Haxaire, J.R. Manouvrier, S. Jan, H. Petiton, J.F. Carpentier, T. Quemerais, C. Durand, D. Gloria, M. Fourel, F. Battegay, Y. Sanchez, E. Batail, F. Baron, P. Delpech, L. Salager, P. De Dobbelaere, and B. Sautreuil: A multi-wavelength 3D-compatible silicon photonics platform on 300 mm SOI wafers for 25Gb/s applications (IEEE Int. Electron Devices Meet., Washington, DC, USA, 2013) p. 353.
5. Y. Urino, N. Hatori, K. Mizutani, T. Usuki, J. Fujikata, K. Yamada, T. Horikawa, T. Nakamura, and Y. Arakawa: First demonstration of athermal silicon optical interposers with quantum dot lasers operating up to 125°C. *J. Lightwave Technol.* **33**, 1223 (2014).
6. Y.A. Vlasov and S.J. McNab: Losses in single-mode silicon-on-insulator strip waveguides and bends. *Opt. Express* **12**, 1622 (2004).
7. R. Orobtchouk, N. Schell, T. Benyattou, and J.M. Fedeli: Compact building block for optical link on SOI technology (European Conf. Integrated Opt., Grenoble, France, 2005).
8. D.K. Sparacin, S.J. Spector, and L.C. Kimerling: silicon waveguide sidewall smoothing by wet chemical oxidation. *J. Lightwave Technol.* **23**, 2455 (2005).
9. W. Bogaerts, R. Baets, P. Dumon, V. Wiaux, S. Beckx, D. Taillaert, B. Luyssaert, J. Van Campenhout, P. Bienstman, and D. Van Thourhout: Nanophotonic waveguides in silicon-on-insulator fabricated with CMOS technology. *J. Lightwave Technol.* **23**, 401 (2005).
10. T. Tsuchizawa, Y. Yamada, H. Fukuda, T. Watanabe, J. Takahashi, M. Takahashi, T. Shoji, E. Tamechika, S. Itabashi, and H. Morita: Microphotonics devices based on silicon microfabrication technology. *IEEE J. Sel. Top. Quantum Electron.* **11**, 232 (2005).
11. F. Xia, L. Sekaric, and Y. Vlasov: Ultracompact optical buffers on a silicon chip. *Nat. Photonics* **1**, 65 (2007).

https://doi.org/10.1557/mrc.2015.84 Published online by Cambridge University Press

12. M. Gnan, S. Thoms, D.S. Macintyre, R.M. De La Rue, and M. Sorel: Fabrication of low-loss photonic wires in silicon-on-insulator using hydrogen silsesquioxane electron-beam resist. *Electron. Lett.* **44**, 115 (2008).
13. T. Tsuchizawa, K. Yamada, T. Watanabe, H. Fukuda, H. Nishi, H. Shinojima, and S. Itabashi: Si photonics platform and its fabrication (Int. Symp. on Adv. Sci. Technol. Silicon Mat., Hawaii, USA, 2008).
14. W. Bogaerts, S.K. Selvaraja, P. Dumon, J. Brouckaert, K. De Vos, D. Van Thourhout, and R. Baerts: Silicon-on–insulator spectral filters fabricated with CMOS technology. *IEEE J. Sel. Top. Quantum Electron.* **16**, 33 (2010).
15. S.K. Selvaraja, G. Murdoch, A. Milein, C. Delvaux, P. Ong, S. Pathak, D. Vermeulen, G. Sterckx, G. Winroth, P. Verheyen, G. Lepage, W. Bogaerts, R. Baerts, J. Van Campenhout, and P. Absil: Advanced 300-mm waferscale patterning for silicon photonics devices with record low loss and phase errors (Opto-Electron. Commun. Conf., Busan, Korea, 2012) p. 15.
16. N. Hirayama, H. Takahashi, Y. Noguchi, M. Yamagishi, and T. Horikawa: Low-loss Si waveguides with variable-shaped-beam EB lithography for large-scaled photonic circuits (Int. Conf. on Solid State Devices Mat., Kyoto, Japan, 2012) p. 530.
17. T. Horikawa, H. Takahashi, M. Seki, and T. Nakamura: Silicon photonic integration by using variable-shaped-beam EB lithography and immersion ArF lithography (Int. Symp. on Photonics Electron. Convergence, Tokyo, Japan, 2012) p. 12.
18. H. Takahashi, M. Toyama, M. Seki, D. Shimura, K. Koshino, N. Yokoyama, M. Ohtsuka, A. Sugiyama, E. Ishitsuka, T. Sano, and T. Horikawa: The impacts of ArF excimer immersion lithography on integrated silicon photonics technology (Int. Conf. on Solid State Devices Mat., Kyoto, Japan, 2012) p. 528.
19. S.K. Selvaraja, P. De Heyn, G. Winroth, P. Ong, G. Lepage, C. Cailler, A. Rigny, K.K. Bourdelle, W. Bogaerts, D. Van Thourhout, J. Van Campenhout, and P. Absil: Highly uniform and low-loss passive silicon photonics devices using a 300 mm CMOS platform (OFC 2014, San Francisco, USA, 2014), Th2A.33.
20. D. Shimura, T. Horikawa, H. Okayama, S.-H. Jeong, M. Tokushima, H. Sasaki, and T. Mogami: High precision Si waveguide devices designed for. 1.31 μm and 1.55 μm wavelengths on 300 mm-SOI (IEEE Int. Conf. on Group IV Photonics, Paris, France, 2014) p. 31.
21. S. Lardenois, D. Pascal, L. Vivien, E. Cassan, S. Laval, R. Orobtchouk, M. Helzmann, N. Bouzzalda, and L. Mollard: Low-loss submicrometer silicon-on-insulator rib waveguides and corner mirrors. *Opt. Lett.* **28**, 1150 (2003).
22. F.P. Payne and J.P.R. Lacey: A theoretical analysis of scattering loss from planar optical waveguides. *Opt. Quantum Electron.* **26**, 977 (1994).
23. T. Barwicz and H.A. Haus: Three-dimensional analysis of scattering losses due to sidewall roughness in microphotonic waveguides. *J. Lightwave Technol.* **23**, 2719 (2005).
24. A. Novack, M. Streshisky, R. Ding, Y. Liu, A.E.-J. Lim, G.-Q. Lo, T. Baehr-Jones, and M. Hockberg: Progress in silicon platforms for integrated optics. *Nanophotonics* **3**, 205 (2014).
25. T. Horikawa and T. Mogami: Ultra-fine Si photonics fabrication technology based on 40-nm-node CMOS process (IEEE Int. Conf. on Group IV Photonics, Vancouver, Canada, 2015) p. 201.
26. T. Horikawa, M. Seki, M. Toyama, K. Koshino, N. Yokoyama, M. Ohtsuka, A. Sugiyama, E. Ishitsuka, M. Yamagishi, and T. Sano: SOI waveguide process(VI) – Waveguide pattern formed by ArF immersion lithography (II) – (IEICE Electron. Conf., Toyama, Japan, 2012) p. 174 [in Japanese].
27. T. Horikawa, D. Shimura, S.-H. Jeong, M. Tokushima, K. Kinoshita, and T. Mogami: The impacts of fabrication error in Si wire-waveguides on spectral variation of coupled resonator optical waveguides. *Microelectron. Eng.* in press doi: 10.1016/j.mee.2015.11.015.
28. T. Barwicz and H.I. Smith: Evolution of line edge roughness during fabrication of high-index-contrast microphotonic devices. *J. Vac. Sci. Technol. B* **21**, 2892 (2003).
29. T. Barwicz, C.W. Holzwarth, P.T. Rakich, M.A. Popovic, E.P. Ippen, and H.I. Smith: Optical loss in silicon microphotonic waveguides induces by metallic contamination. *Appl. Phys. Lett.* **92**, 131108 (2008).
30. K. Kinoshita, T. Horikawa, D. Shimura, H. Takahashi, and T. Mogami: *Study of O3-TEOS SiO_2 Cladding for Silicon Photonics Devices* (GEC/ICRP/SPP, Honolulu, USA, 2015), NR2.00002.
31. D.K. Sparacin: Process and design techniques for low loss integrated silicon photonics. PhD thesis, MIT, 2006, pp. 84–106.

https://doi.org/10.1557/mrc.2015.84 Published online by Cambridge University Press